Journal of Oncology Research and Treatments

Wang and Yang, J Oncol Res Treat 2020, 5:2

Original Article Open Access

Multi Slice Spiral CT Manifestations and Comparative Analysis of Different Pathological Classifications of Lung Infiltrating Adenocarcinoma

Minke Wang and Hai Yang*

Radiology Department, Taizhou Enze Medical Center (Group) Enze Hospital, Taizhou 18000, China

Abstract

Objective: To review and analyze the correlation between Multi Spiral Computed Tomography (MSCT) findings of lung infiltrating adenocarcinoma and different new pathological classifications, and to evaluate the classification of Invasive Adenocarcinoma (IAC) from the perspective of imaging, so as to help the clinical formulation of treatment plan and prediction of prognosis.

Methods: A total of 137 patients with pulmonary infiltrative carcinoma confirmed by operation and pathology and with complete MSCT data from January 2014 to June 2019 in our hospital were collected and sorted. According to the new pathological classification, Lepidic Predominant Adenocarcinoma (LPA), Acinar Predominant Adenocarcinoma (APA) and Papillary Predominant Adenocarcinoma (PPA) were classified as the group with Moderate high differentiation (n=76), Micorpapillary Predominant Adenocarcinoma (MPA) and solid predominant adenocarcinoma with mucin production as the group with low differentiation (n=61). The MSCT characteristics of the two groups were classified and analyzed for statistical analysis.

Results: The length, CT value and arteriovenous CT value of the lesions in the low differentiation group were higher than those in the moderate high differentiation group, and there was statistically significant difference between the two groups ($P<0.05$), but there was no significant difference between the two groups in the lesion boundary, blood vessel change, bronchi inflation sign and burr sign ($P>0.05$).

Conclusion: MSCT signs of infiltrating adenocarcinoma are helpful to differentiate different pathological subtypes.

Keywords: Lung infiltrating adenocarcinoma; Pathological classification; Multi spiral computed tomography

Introduction

Lung cancer has become the malignant tumor with the highest morbidity and mortality, among which Non-Small Cell Lung Adenocarcinoma (NSCLC) accounts for 80% of primary lung cancer [1]. Recent years, the incidence of lung adenocarcinoma has gradually increased, and it has become the most common type of lung cancer, among which Invasive Pulmonary Adenocarcinoma (IAC) has a poor prognosis, a higher probability of metastasis and a lower survival rate. In 2015, the International Association for the Study of Lung Cancer, the American Thoracic Society and the European Respiratory Society (IASLC/ATS/ERs) jointly launched an international multidisciplinary classification of lung adenocarcinoma. The invasive adenocarcinomas were divided into five categories: Lepidic Predominant Adenocarcinoma (LPA, formerly non-mucinous BAC growth pattern, infiltration range >0.5cm), Acinar Predominant Adenocarcinoma (APA), papillary predominant adenocarcinoma (PPA), micorpapillary predominant adenocarcinoma (MPA), and solid predominant adenocarcinoma with mucin production [2]. According to Yang Xin et al., it is a simple and effective way to grade adenocarcinoma according to its main structure; there are great differences in clinical intervention and prognosis among different pathological types of adenocarcinoma [3]. Studies have shown that micropapillary predominant adenocarcinoma and solid predominant adenocarcinoma with mucin production have higher recurrence and metastasis rates and lower postoperative survival rates, while acinar predominant adenocarcinoma and papillary predominant adenocarcinoma have better prognosis [4]. Oshizawa and other data showed that the 5-year disease-free survival rate of I patients with micorpapillary predominant adenocarcinoma was only 67%. stage I patients with lepidic predominant adenocarcinoma have better prognosis, and the 5 years survival rate was up to 90%. Compared with lepidic predominant adenocarcinoma, patients with micropapillary or solid predominant adenocarcinoma may be more suitable for total lobectomy [4-7]. Zhu Meng et al. showed that the 5-year progression free survival rate and 5-year overall survival rate of LPA patients were 100%, while the 5-year progression free survival rate of MPA and entity type patients was 50.0% and 61.5% [8]. It had been reported in the literature that metastasis can occur early in patients with MPA, therefore, PET-CT was recommended for lung nodules or masses that are considered MPA [9].Therefore, accurate preoperative identification of the tumors' differentiation degree is essential for formulating treatment strategies and predicting disease prognosis.

At present, it is still the gold standard to judge the subtype of invasive adenocarcinoma by pathological tissue. But routine puncture biopsy, including intraoperative freezing due to less pathological quantity and insufficient experience, is often difficult to accurately determine the specific subtype [10]. In general, we can type accurately after complete resection of the tumor, which is difficult for surgeon to make decision in surgery. And whether it's biopsy or surgery, it's invasive. Some patients cannot tolerate. With the development of imaging technology and the improvement of imaging diagnosis, it is possible to predict the subtype of invasive adenocarcinoma before operation.

***Corresponding author:** Hai Yang, Radiology Department, Taizhou Enze Medical Center (Group) Enze Hospital, Taizhou 18000, China, Tel: +86057685120120; E-mail: yanghai@enzemed.com

Received April 09, 2020; **Accepted** May 15, 2020; **Published** May 22, 2020

Citation: Yang H, Wang M (2020) Multi Slice Spiral CT Manifestations and Comparative Analysis of Different Pathological Classifications of Lung Infiltrating Adenocarcinoma. J Oncol Res Treat 5: 146.

The authors retrospectively analyzed the clinical and imaging characteristics of different pathological classifications of pulmonary invasive adenocarcinoma, aiming to explore the correlation between clinical and CT signs of pulmonary invasive adenocarcinoma and pathological classification, in order to predict the degree of lesion differentiation before surgery, and to help surgeons formulate preoperative treatment plans.

Data and Methods

Clinical data

Retrospectively collect the CT, pathological and clinical data of 137 patients with pulmonary invasive adenocarcinoma confirmed by surgery and pathology in our hospital from May 2014 to May 2019, including 83 males and 54 females, aged 37-94 years, with an average age of (62.2+10.5) years, totaling 137 lesions. Patient inclusion criteria: ① pathologically confirmed invasive adenocarcinoma of the lung; ② perform CT examination before surgery, and the interval between preoperative examination and surgery was less than 1 month; ③ CT examination images included 1 mm or less thick and thin layers of images without motion artifacts or metal artifacts affecting nodule observation; ④ lesions had not received any anti-tumor treatment before CT scan. Exclusion criteria: ① poor image, affecting the observer; ② patients received anti-tumor treatment before surgery. Finally, 137 invasive adenocarcinomas were enrolled.

Classification criteria: According to the new classification of pathology and prognosis [2-10]. The LPA+APA+PPA were classified into the high differentiation group, with a total of 76; the solid-dominant version with mucin production+MPA were classified into the low differentiation group, with a total of 61 were analysis statistically.

CT scanning methods

All subjects underwent High Resolution CT (HRCT) within 1 month before surgery and were scanned on high Definition Discovery CT750HD (GE Healthcare). Scanning parameters: pitch 0.984, collimation width 32mm×1.25mm, scanning thickness 5mm, tube voltage 120kV, automatic tube current, FOV 35cm, X-ray tube speed 0.6s/r. Target scanning was performed on the basis of conventional HRCT scanning, with pitch of 0.984, collimation width of 64 mm×0.625 mm, scanning thickness of 0.625mm, tube voltage of 140 kV, automatic tube current, FOV20cm, and rotation speed of 0.6s/r. Lung window width 1500Hu, window position - 450Hu, mediastinal window width 400Hu, window position 40Hu. All images were obtained after end-inspiratory closure [11].

Image analysis

Send the scanning data to the post-processing workstation for image analysis. Two radiologists who have been engaged in chest CT diagnosis for more than 10 years read the films independently by blind method. If they had different opinions, the third deputy director physician sill reached an agreement after review. According to the prognosis and survival rate, 137 lesions were divided into two groups: high differentiation (lepidic+papillary+acinar) and low differentiation (micropapillary+solid). Because a few lesions had no complete arteriovenous phase image (13/61), it was performed on the plain scan image to better compare the morphological manifestations between the two groups. Assessment items included: ① nature of lesions, which were divided into pure ground glass nodules, mixed ground glass nodules and solid nodules; ② length diameter, measuring the maximum diameter of lesions on three-dimensional images (unit: cm); ③ density, ROI area = 10 mm2, avoiding the interference of blood vessels, bronchial shadow and vacuoles by multiplanar imaging, and measure three times at different locations of lesions, take the average value (unit: Hu); ④ shape, divided into circular or oval, irregular; ⑤ edge, divided into smooth, lobulated, burr, burr+lobulated; ⑥ Vascular changes, distortions, thickening or aggregation of blood vessels entering or passing through the tumor; ⑦ Tumor-lung interface, divided into clear and unclear; ⑧ Other signs, including vacuole sign, air bronchus sign, pleural depression sign [12].

Data measurement and collation

Manually set the region of interest (ROI) for measurement. ROI placement avoided the obvious necrosis, calcification, cystic degeneration and bleeding of the tumor. ① 1CT value and enhancement amplitude (enhance arterial and venous phase CT value): Measure and record CT values after plain and enhanced CT respectively. ② Record the longest diameter of the tumor, the clear or unclear of the lung tumor interface, shape, density, edge, vascular changes, pleural depression, vacuole sign, air bronchus sign, etc.

Statistical analysis

Use Medcalc statistical software (Version 19-64-bit, https://www.medcalc.org) to analyze the obtained data. Independent sample t-test was used for variable data between two groups. If the variables satisfied a normal distribution, T test was used to compare the groups. Otherwise, the Mann-Whitney U test was used to compare the groups. Differences in sex composition, vacuole sign, air bronchus sign, pleural depression sign, vascular changes, lesion edge and tumor-lung interface among different differentiation groups were compared by $\chi 2$ test.

The age of patients and the length and destiny of lesions were expressed as $\chi(-)\chi\pm s$. The CT values of each period between the two groups were not normal distribution, which was tested by Mann Whitney U. The morphology and CT value of each phase between the middle and high differentiation and low differentiation groups were analyzed by Receiver Operating Characteristic Curve (ROC). $P<0.05$ was statistically significant.

Results

The clinical data of 137 lesions and the statistical analysis results of CT plain scan image were shown in Table 1. 76 cases in the moderate high differentiation group and 61 cases in the low differentiation group. The mean age of the two groups was 60.79 ± 10.28 and 63.82 ± 10.72, respectively, P=0.117; the length of the two groups was 17.3 ± 7.5mm and 26.5 ± 15.8mm, respectively, The difference was statistically significant (P=0.0001); there was no statistically significant difference between the two groups in gender, tumor lung interface and shape, vascular change, pleural depression, vacuole sign, air bronchogram pathological nature, pathological edge; age, gender, tumor lung interface and shape, vascular change, pleural depression, vacuole sign, air bronchogram between the two groups. There were significant differences in length, lesion nature and lesion edge ($P<0.05$). In the moderate high differentiation group, there were 23 cases (30%), 14 cases (18%), 15 cases (20%) of burrs, 24 cases (32%) of burrs + lobes; in the low differentiation group, there were 6 cases (10%), 22 cases (36%), 5 cases (8%), 28 cases (46%) of burrs + lobes; The area under curve (AUC) values were 0.59, 0.68 and 0.85, respectively, The sensitivity was 90.2%, 60.7%, 90.2%; the sensitivity was 30.3%, 71.1%, 78.9%; there was significant difference between the two groups in three-phase CT value (All $P<0.0001$, as shown in Table 2), ROC curve showed that the CT value of each phase has a good diagnostic efficiency between the high

Clinical features	Moderate high differentiation (n=76)	Low differentiation (n=61)	P value
Age	60.97 ± 10.28	63.82 ± 10.72	0.117[b]
Sex (n)			
Male	41 (54%)	42 (69%)	0.82
Female	35 (46%)	19 (31%)	
Length (mm)	17.3 ± 7.5	26.5 ± 15.8	0.0001[b]
Vacuole sign(n)			
Yes	19 (25%)	10 (16%)	0.293[a]
No	57 (75%)	51 (84%)	
Air bronchus sign(n)			
Yes	21 (28%)	22 (36%)	0.292[a]
No	55 (72%)	39 (64%)	
Vascular changes(n)			
Yes	63 (83%)	50 (82%)	1.000[a]
No	13 (17%)	11 (18%)	
Lesion edge (n)			
Smooth	23 (30%)	6 (10%)	0.0014[a]
Lobulation	14 (18%)	22 (36%)	
Spiculation	15 (20%)	5 (8%)	
Lobulation+spiculation	24 (32%)	28 (46%)	
Lesion nature (n)			
Solid	16 (21%)	55 (90%)	<0.0001[a]
Mixed ground glass	51 (67%)	6 (10%)	
Pure ground glass	9 (12%)	0	
Lesion morphology(n)			
Circular	26 (34%)	32 (52%)	0.06[a]
Irregular	38 (50%)	19 (32%)	
Ellipse	12 (16%)	10 (16%)	
Lung tumor interface(n)			
Clear	62 (82%)	56 (92%)	0.086[a]
Unclear	14 (18%)	5 (8%)	
Pleural indentation (number)			0.062[a]
Yes	38 (50%)	22 (36%)	
No	38 (50%)	39 (64%)	
CT value (Hu)			
Plain scan	-220.6757 (-271.0332 to -170.3181)	-8.1921 (-27.9378 to 11.5535)	<0.001[b]
Arterial phase	173.4632 (-225.0740 to -121.8523)	29.7663 (10.3112 to 49.2213)	<0.001[b]
Venous l phase	-177.2203 (-227.8775 to -126.5630)	35.9569 (16.8356 to 55.0782)	<0.001[b]

[a]χ^2 value, [b]F value.

Table 1: Clinical data of moderate high differentiation and low differentiation groups.

Variable	AUC	SE[a]	95% CI[b]	Sensitivity	Specificity	P value
Lesion edge	0.592	0.0466	0.505 to 0.675	0.902	0.303	0.049
Length	0.683	0.0466	0.598 to 0.760	0.607	0.711	<0.01
Lesion nature	0.851	0.0293	0.781 to 0.906	0.902	0.789	<0.01
Plain scan (Hu)	0.829	0.0379	0.749 to 0.892	73.2	81.6	<0.0001
Arterial phase (Hu)	0.780	0.0421	0.695 to 0.851	89.6	68.4	<0.0001
Venous l phase (Hu)	0.836	0.0379	0.756 to 0.897	91.7	72.4	<0.0001

[a]DeLong et al., 1988, [b]Binomial exact

Table 2: Significant difference between the two groups in three-phase.

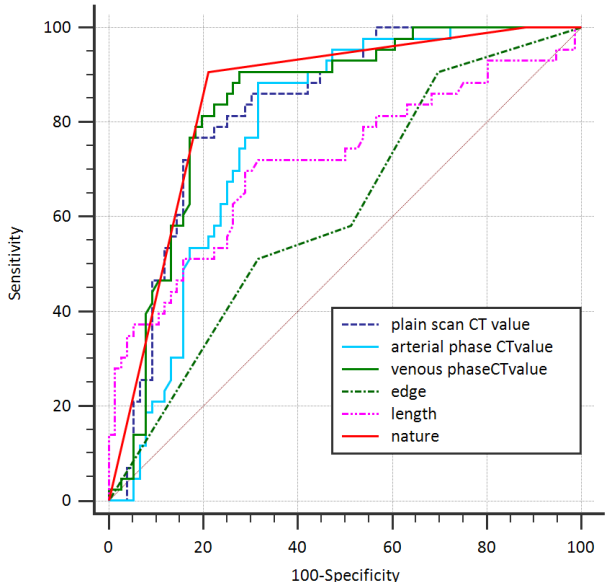

Figure 1: ROC curve shows that the edge, nature and length of the lesion and CT values of plain scan, arterial phase and venous phase have a good diagnostic effect on the moderate high differentiation and low differentiation.

Comparison of different phases	P value
Plain scan ~ arterial phase	P=0.0779
Plain scan ~ venous phase	P=0.7836
Arterial phase ~ venous phase	P=0.0313

Table 3: Pairwise comparison of ROC curves.

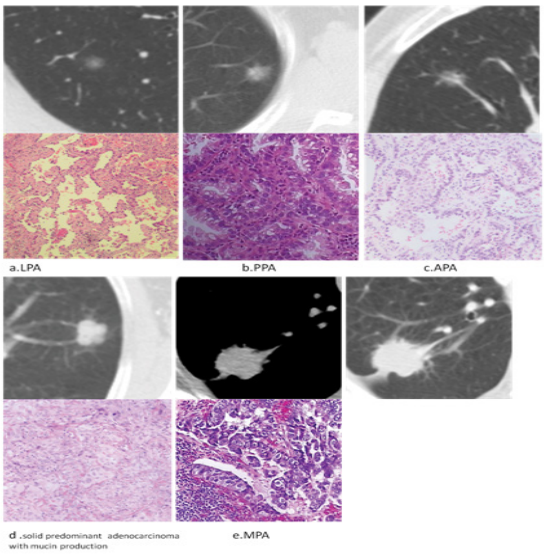

Figure 2: A,a, male, 48 years old, (upper right) invasive pulmonary adenocarcinoma (lepidic predominant adenocarcinoma); B,b, male, 65 years old,(left upper) invasive pulmonary adenocarcinoma (papillary predominant adenocarcinoma); C,c, male, 60years old, (upper right) invasive pulmonary adenocarcinoma(acinar predominant adenocarcinoma). A-C showed mixed ground glass shadows, low density, smooth edge, shallow or inconspicuous lobulation. D,d, male, 59 years old,(left upper) invasive pulmonary adenocarcinoma(solid predominant adenocarcinoma); E,F,e, male, 60years old, (upper right) invasive pulmonary adenocarcinoma(micorpapillary predominant adenocarcinoma). D-F showed solid lesions with obvious burrs, deeper lobulation, and more obvious adjacent pleural traction depression.

and low differentiation groups (Figure 1); the AUC value of the plain scan was 0.829, the sensitivity and specificity were 73.2% and 81.6% respectively, the sensitivity and specificity of the venous phase CT value were 91.7% and 72.4%, the sensitivity and specificity of the arterial phase were 89.6% and 68.4% respectively; The AUC value for the venous phase (0.836) was higher than that for the arterial phase (0.780), $P<0.05$ (Figure 1). There was no significant difference between plain scan and venous phase (Table 3). There were also some differences in morphology and pathology among pathological subtypes of invasive adenocarcinoma (Figure 2).

Discussion

Our study found that lesion nature, edges, and length diameter were independent predictors of low differentiation and moderate high differentiation IAC. The imaging manifestations of the lesions are closely associated with histopathological changes. LPA, grows in an appendicular fashion along the alveolar wall, but at least one component of the infiltrative carcinoma under the visual field has a maximum diameter of ≥ 5 mm, or the tumor invades the vasculature, lymphatic vessels, or pleura or presents tumor necrosis. APA, a round or oval gland with a central ductal lumen, PPA consists mainly of branching papillae with a fibrous vascular axis [13]. Tumors with these three growth styles are limited by surrounding structures, having relatively low malignancy and slow proliferation, so early lung cancer is more likely to show grinding glass or mixed grinding glass-like changes such as alveolar infiltration (about 79%), smaller lesions and smooth edge (about 30%). However, MPA, a papillary cell cluster without fiber vascular axis, connected with or separated from the alveolar wall, or in ring like adenoid structure "floating" in the alveolar space, vascular and interstitial infiltration is common, sometimes sand bodies can be seen ;solid-type adenocarcinoma with mucus-producing type, lacks of recognizable adenocarcinoma structure, and tumor shows 100% solid growth; therefore, these two types of lesions lack obvious fibrous vascular structure or recognizable adenocarcinoma structure, so they are more likely to show realistic changes (about 90%), the lesions are often larger, more likely to show signs such as lobules and burrs, and only 10% of the smooth edge [14,15]. Yanju et al. also showed that the main lung adenocarcinoma of micropapillary type basically had the typical manifestations of lobulation sign, hairpin sign and pleural depression sign of peripheral lung cancer [16]. Aherne Emily A et al. showed that tumor size was an independent risk factor for death and recurrent metastasis in patients, which is consistent with our results showing a significantly larger mass in the low differentiation group than in the moderate high differentiation group [17].

We found enhanced diagnostic efficacy in the venous phase to be higher than in the arterial phase. The authors believe that this is related to the permeability of tumor vessel wall. Zhang MM believes, according to the two-compartment model theory of tumor enhancement, the enhancement of early mass after contrast injection is mainly determined by intravascular contrast agent [18]. With the passage of time, the contrast agent gradually enters the extravascular interstitial structure through the capillary wall. Therefore, the author believes that intravascular contrast agents infiltrate the extravascular stroma from the vascular phase through the incomplete basement membrane. This process is also more reflective of the destruction of the surrounding stroma of the mass and more likely to reflect vascular permeability. Our results corroborated the greater vascular permeability, easier invasion, infiltration, and early metastasis of the low differentiation group.

There were some limitations in this study. First, the study was retrospective study, and the enrolled cases were all surgical cases, so there was a selection bias. Secondly, the small sample size of pathological changes in the poorly differentiated group (especially MPA) is related to the strict inclusion of MPA and solid type as the dominant components in the grouping. In the subsequent study, the cases with micropapillary and entity components (non dominant) will be further included in the study. Finally, there might be some errors in the measurement of CT values of some nodules with less uniform density, but the density of the low differentiation group was significantly higher than that of the middle and high differentiation group, so the effect was relatively small.

Conclusion

In conclusion, our study suggests that solid lesions, larger lesion margin burrs, and foliated lesions are more prone to low differentiation. Whereas smaller frosted glass or mixed frosted glass lesions with smooth edges were more likely to be moderately highly differentiated, suggesting a better postoperative prognosis.

References

1. Zhonghua B, Li X. Za Z (2018) Expert consensus on diagnostic pathology of ROS1-positive non-small cell lung cancer. Chinese Journal of Pathology 47: 248-251.
2. Fang J, Jiang GN (2016) Impact of the new classification of lung adenocarcinoma on surgical treatment in the 2015 WHO classification system for lung cancer. Chinese Journal of Thoracic and Cardiovascular Surgery 32: 688-691.
3. Yang X, Lin DM (2016) Changes in the histological classification of lung cancer and its clinical significance in the 2015 WHO. Chinese Journal of Lung Cancer 19: 332-336.
4. Zhou LX, Chen KZ, Yang F, Liao Y, Sun K, et al. (2014) Analysis of risk factors for postoperative recurrence of stage T1aN0M0 invasive lung adenocarcinoma. Chinese Journal of Experimental Surgery 31:1639-1641.
5. Eguchi T, Yoshizawa A, Kawakami S, Kumeda H, Umesaki T, et al. (2014) Tumor size and computed tomography attenuation of pulmonary pure ground-glass nodules are useful for predicting pathological invasiveness. PLoS One 9: 349-356.
6. Zhang L. Imaging and related research of lung adenocarcinoma based on IASLC/ATS/ERS multidisciplinary new classification .Peking Union Medical College. 2014.
7. Qiu Yangbo, Mao Feng, Zhang Hui, Shen-Tu Yang (2018) Factors influencing the progression trend of early lung cancer and CT findings. Chinese Journal of Lung Cancer 21: 793-799.
8. Zhu M, Sun WG (2018) Different pathological type period the survival condition of patients with lung adenocarcinoma. China Medicine and Pharmacy 8: 200-203.
9. Ren JF, Zhou JY, Ding W, Zhong B, Zhou J (2014) Clinicopathologic and imaging features of lung adenocarcinoma with micropapillary structure. Chinese Journal of Oncology 36: 282-286.
10. Zhang J, Shao J, Zhu L (2015) 2015 edition of WHO lung tumor classification interpretation. Chinese Journal of Pathology 44: 619-624.
11. Yang H, Lin X, Chen Y, Zheng H, Wu J, et al. (2016) Window technology to distinguish pure ground-glass density lung in situ adenocarcinoma from microinfiltrating. Zhejiang Practical Medicine 21: 398-401.
12. Yang H, Chen Y, Lin X (2018) Correlation between CT features and pathological types of Pure ground glass lung adenocarcinoma with a maximum diameter of 1-3cm. Chinese Journal of General Practice 16: 969-973.
13. Huang SF (2011) Interpretation of the international association for lung cancer research/American thoracic society/European respiratory society international multidisciplinary classification of lung adenocarcinoma (2011 edition). Chinese Journal of Pathology 40: 793-796.
14. Chen ZW, Teng XD (2016) Classification of lung tumors histology in WHO 2015. Chinese Journal of General Practice 23: 60-64.
15. Zhou XJ, Liu B (2011) Interpretation of the 2011 international multidisciplinary classification of IASLC/ATS/ERS lung adenocarcinoma. Chinese Journal of Clinical and Experimental Pathology 27: 801-810.

16. Li YJ, Ye ZX, Song Q (2015) Features of multislice spiral computed tomography in micropapillary-predominant lung adenocarcinomas. Chinese Journal of Clinical Oncology 42:912-915.

17. Aherne EA, Plodkowski AJ, Montecalvo J, Hayan S, Zheng J, et al. (2018) What CT characteristics of lepidic predominant pattern lung adenocarcinomas correlate with invasiveness on pathology?. Lung cancer 118: 83-89.

18. Zhang MM, Zhou H, Zhou Y (2005) Angiogenic CT study of lung cancer and MR perfusion imaging. Radiologic Practice 20: 286-290.